

Rayleigh Waves in an isotropic Body with Deep Periodic Grooves

Eugeniusz DANICKI

Institute of Fundamental Technological Research

Polish Academy of Sciences

Pawińskiego 5B, 02-106 Warszawa, Poland

e-mail: edanicki@ippt.gov.pl

(received September 2, 2009; accepted November 25, 2009)

Bragg scattering of waves propagating in a periodically disturbed substrate is widely applied in optics and micro-acoustic systems. Here, it is studied for Rayleigh waves propagating on a periodically grooved elastic substrate. Practically applied groove depth in the Bragg grating reflectors does not exceed a few percent of the Rayleigh wavelength. Here, the analysis is carried out for periodic grooves of larger depth by applying the elastic plate model for the groove walls. The computed results show that the surface wave existence and reflection depends strongly on both the groove depth and period, and that there are limited domains of both for practical applications, primarily in comb transducers of surface waves.

Keywords: surface acoustic waves, Bragg reflection, comb transducers.

1. Introduction

Wave scattering and propagation on a grooved surface of elastic body was the subject of investigations for years (BREHOVSKICH, 1957; GLASS, MARADUDIN, 1983). Most research works concerned shallow grooves (BIRIUKOV *et al.*, 1995; DANICKI, 1984) where the perturbation method was applicable. Here, we analyze deep groove-gratings, or equivalent systems of periodic teeth (the groove walls), where perturbation theory cannot be applied.

In (DANICKI, 2008), we proposed treating elastic teeth as pieces of an elastic plate. The concept was proven for shallow grooves; the results nicely converged to these obtained by perturbation analysis. Next two sections shortly outline the applied approach (DANICKI, 2008) for evaluation of the tooth harmonic impedance which is subsequently used in formulation of the boundary-value problem under consideration. Elevated teeth are typically applied in ultrasonic comb transducers of surface waves (QUARRY, ROSE, 2002; VIKTOROV, 1967;

DANICKI, 2000b). The analysis presented here may help to improve their efficiency.

The following sections present the computed spatial frequency of the surface wave which takes complex values when Bragg reflection occurs. Two most interesting cases are presented: for period of grooves smaller than half of the Rayleigh wave-length λ_R , which is the case exploited in Bragg reflectors of Fabry–Perrot resonators in micro-acoustic devices (BIRIUKOV *et al.*, 1995; DANICKI, 1984), and the case of teeth period close to λ_R , applied in comb transducers (DANICKI, 2002). In the latter case, the surface wave spatial frequency takes complex values for two reasons: due to the Bragg reflection and due to the scattering into bulk waves in the substrate. In comb transducers, the surface wave decaying (described by imaginary part of its spatial frequency) should have rather moderate values in order to allow many teeth of the comb to contribute to the transducer output. Such comb optimization is not a trivial task.

2. Tooth harmonic impedance

Standard notations for mechanical fields are applied: u_i , T_{3i} , $i = 1, 3$ are correspondingly the displacement and stress tensor components. The field is assumed to be independent of y -axis and its general harmonic form at the substrate surface $z = 0$ is

$$F(x) \exp(-j2\pi pz),$$

neglecting the time-harmonic term $\exp(j2\pi ft)$, where p is the spatial frequency of the plate mode propagating along axis z ; the mode shape in the plate cross-section is $F(x)$.

A tooth of rectangular cross-section is a d -long piece of a plate of thickness w (Fig. 1; its upper end is assumed to be stress-free). All propagating modes (having real $p = p_i$) existing in the plate, and finite number of the lowest evanescent modes (decaying at $|z| \rightarrow \infty$) are accounted for in the applied mode-matching analysis (BESSERER, MALISHEVSKY, 2004). The impedance relation for the wave-field at the bottom cross-section $z = 0$ is evaluated using the method presented in (DANICKI, 2008):

$$T_{3i}^{(n)} = H_{il}^{(nm)} u_l^{(m)}, \quad (1)$$

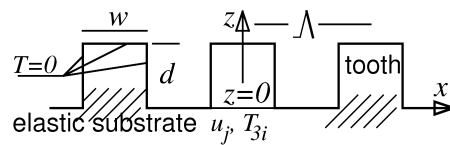


Fig. 1. Periodic system of teeth. In computations, elastic substrate is characterized by longitudinal and shear spatial frequencies: $k_t = 1$ and $k_l = 0.4746$, respectively and $k_R = 1/\lambda_R = 1.069$; $w = \lambda_R/4$.

where $i, l = 1, 3$ and n, m are the orders of natural (w -base) Fourier expansion of the field in the plate cross-section $z = 0$:

$$\begin{bmatrix} u_l \\ T_{3i} \end{bmatrix}_{z=0}(x) = \sum_n \begin{bmatrix} u_l^{(n)} \\ T_{3i}^{(n)} \end{bmatrix} e^{-jn2\pi Wx}, \quad W = 1/w \quad (2)$$

(the time-harmonic term $\exp j2\pi ft$ is dropped).

In the presented examples, $w = 0.25\lambda_R$ where $\lambda_R = 1/k_R$ is the Rayleigh wave-length in aluminium. Moderately large number of 82 plate modes (including four existing propagating modes with spatial frequency $\pm p_{1,2}$) was used in order to obtain the matrices $\mathbf{H}_{il} = [H_{il}^{(nm)}]$ with good accuracy.

3. The boundary-value problem

For a Λ -periodic system of teeth on an elastic half-space $z < 0$, the surface wave-field at the contact plane $z = 0$ is expanded into Bloch series:

$$\begin{bmatrix} u_j \\ T_{3i} \end{bmatrix}_{z=0}(x) = \sum_k \begin{bmatrix} u_j^{(k)} \\ T_{3i}^{(k)} \end{bmatrix} e^{-j2\pi(r+kK)x}, \quad K = 1/\Lambda, \quad (3)$$

where $r < K/2$ is the surface wave spatial frequency for evaluation.

There is a simple transformation between the representations of the surface displacements on the tooth end, Eq. (2), and the substrate surface, Eq. (3), both contacting in the Λ -periodic domain $x \in (-w/2, w/2)$ (DANICKI, 2008):

$$u_i^{(n)} = C_{nk} u_i^{(k)}, \quad C_{nk} = \frac{\sin \pi(n - r/W - kK/W)}{\pi(n - r/W - kK/W)}. \quad (4)$$

In the applied notations, the subscripts (n) and (k) indicate the wave-field expansion over w or Λ domains according to Eq. (2) and Eq. (3), respectively.

Concerning the surface traction, we know that it is zero between the teeth, and must be continuous in the contact domain. This yields the following transformation:

$$\begin{bmatrix} T_{3j}^{(k)} \end{bmatrix} = \frac{w}{\Lambda} \mathbf{C}^T \begin{bmatrix} T_{3j}^{(n)} \end{bmatrix}, \quad (5)$$

which, accounting for Eq. (1) and applying the Green function \mathbf{G} (DANICKI, 1984; 2008) for the substrate $z < 0$:

$$u_i^{(k)} = G_{ij}(p) T_{3j}^{(k)}, \quad p = r + kK, \quad (6)$$

results in the following r -dependent system of homogeneous equations:

$$\begin{aligned} \mathbf{M}[u_i^{(n)}] &= 0, \\ \mathbf{M} &= \mathbf{I} - (w/\Lambda) \mathbf{G} \mathbf{C}^T \mathbf{H} \mathbf{C}. \end{aligned} \quad (7)$$

The condition for r is:

$$\det \mathbf{M} = 0, \quad (8)$$

and r becomes complex-valued in two cases: 1) in the stop-band where the standing surface wave is composed of two evanescent modes decaying on their propagation path due to the Bragg reflection from the teeth, and 2) when the surface wave is a leaky wave that sheds its energy into bulk waves propagating in the substrate; this is the Bragg scattering into the bulk waves.

In the first case, the solution to r will have the known ideal form:

$$r \sim \sqrt{(f - f_1)(f - f_2)}, \quad (9)$$

where $f_{1,2}$ are stopband frequencies between which r takes complex values (r is a real outside stopband). These frequencies transform to $K_{1,2}$ or $d_{1,2}$ in the conditions applied in this paper, where f is assumed constant and either varying K or d replaces f in the above formula. This ideal form of r may be somehow distorted but generally, the spatial frequency r takes the real value outside the corresponding domains (d_1, d_2) (see case D in Fig. 2, thin lines) or (K_1, K_2), naturally if no bulk waves are scattered into the substrate. That is, if no Bloch components of the expansion (3) have the spatial frequency in the domain $(-k_t, k_t)$, below the cut-off spatial frequency of bulk waves in the substrate. Taking into account the Bragg condition: $2r \approx K$, this requires that $K > 2k_t$.

For $K < 2k_t$, we may deal with the second case mentioned above, where surface waves are scattered by teeth into bulk waves in the substrate, causing the surface wave energy “leaking” into bulk of the body. This is the reason that r takes complex values outside the supposed stopband; in the stopband, this phenomenon contributes to the imaginary part of r .

4. Discussion of the case $K > 2k_t, r \sim K/2$.

Bragg reflections occur at $r \approx K/2$. The stopband edges are defined by values of $K = K_s$ where imaginary part of r vanishes, hence when the solution to r is exactly $K_s/2$. The values of K_s are relatively easy for evaluation from Eq. (8); the results are shown in Fig. 2, where thick lines present the dependence of K_s on the teeth height d relative to the wave-length of transverse wave $\lambda_t = 1/k_t = 1$. Two families of curves $K_s(d)$ differ by their slopes; their periods are approximately $1/p_i$ where $p_1 = 1.45$ and $p_2 = 0.57$ are the wave-numbers of propagating plate modes. The ‘proper Bragg reflection’ occurs in the domains of d (or K) between stopband edges set by the curves belonging to different families, like in the presented $r(d)$ in the case D (solid and dashed thin lines present correspondingly the imaginary and real parts of r ; vertical axis $r' = r - K/2$). In other cases, r varies very rapidly around $K_s(d)$ (thin lines in cases B and C for $K = 2.3$ and also in the case A for $K = 2.5$, in which cases $\text{Im}\{r\}$ grows rapidly), there are not pairs of stopband edges, and thus r does not follow Eq. (9) that characterizes the ‘proper

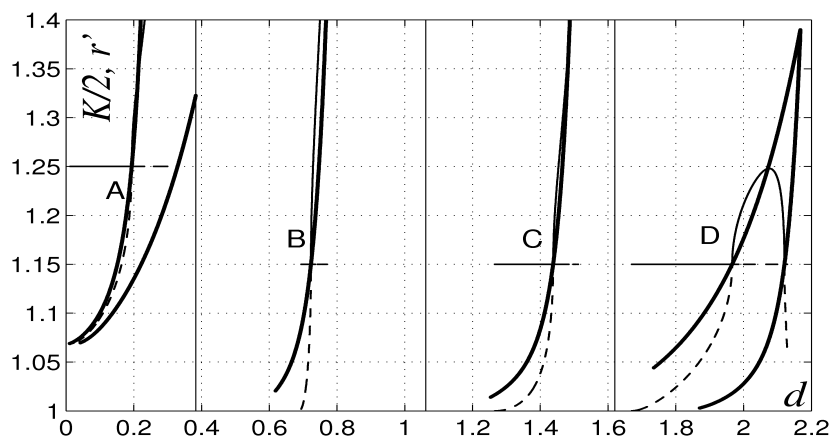


Fig. 2. Stopband edges $K = K_s$ dependent on the teeth height d . Two periodic families of curves $K_s(d)$ can be discerned by their slopes; applicable stopbands reside between them.

Bragg reflection'. Thin vertical solid lines in Fig. 2 mark the values of d where $\det\{H\} = 0$; there are resonances of a free tooth (PAGNEUX, 2006). Other curves are discussed below.

For given $K = 2.3$, the dependence of r on d is presented in Fig. 3. For Bragg reflection, the ideal drawing of complex solutions to r would be a half-circle, Eq. (9). However, in large domain of teeth height, from nearly zero up to almost $10w = 2.5\lambda_R$, $r(d)$ satisfies this expectation only in two domains marked in Fig. 2 by letters A and D (between $K_s(d)$ of different slopes). If two curves K_s of different slopes cross each other (see case D), the stopband width and the Bragg reflection vanish, hence the wave propagates freely like a Rayleigh wave. Having spatial frequency $r = K/2 \gg k_R$, it is however a much slower wave.

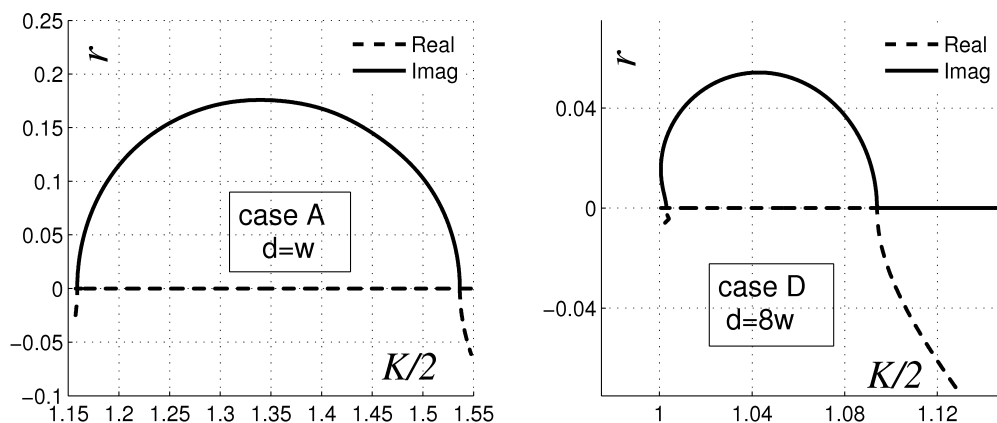


Fig. 3. Solutions to $r(K)$ for given d , presenting close to ideal semicircles of imaginary parts of r in stopbands; cases A and B correspond to Fig. 2.

It is seen in Fig. 2 that drawings of real values of r (thin dashed lines) end at $r = k_t$. Its continuation supposedly enters the domain of leaky waves, $r < k_t = 1$. The imaginary values grow fast to very high values (except the case D). The above discussion may be concluded that only two domains of d , indicated by A and D in the discussed domain $(0, 10)w$, may find practical applications in surface wave Bragg reflectors, with their performances depending on the applied teeth period $2\pi/K$. It is worth to remark here that both r and $K - r^*$ are the solutions to Eq. (8); the figures present one branch only.

Figure 3 presents the dependence of $r(K)$ for two chosen values of d : $d = w$ and $8w$, residing in the ‘proper Bragg reflection’ domains marked by A and D in Fig. 2. Although the presented stopband for the case A ($d = w$) is wider as compared to the case D, ($d = 8w$), the stopband there can also be obtained wider for higher d . Computations for other values of d in the case A have shown that the semicircle drawing of $\text{Im}\{r\}$ is obtained only for small d residing below the left curve $K_s(d)$ presented in Fig. 2. For higher K , $\text{Im}\{r\}$ behaves like in the case B and C, as discussed above for $K = 2.5$. This indicates that choosing proper values of d for applicable Bragg reflectors may be tricky, requiring careful analysis.

5. Case $K \sim k_R$, $r \approx 0$.

In the case $K \sim k_R$ ($\Lambda \sim \lambda_R$), the Bloch series (3) includes the wave component having wave-number in the interval $(-k_r, k_t)$, that is in the area of projection of bulk wave-vectors $\vec{k}_{l,t}$ on x -axis. Any surface stress caused by teeth on the substrate surface $z = 0$ will excite these bulk waves at the cost of propagating surface wave power. This is the reason that the wave-number of surface wave becomes complex-valued in such cases.

Figure 4 presents the evaluated wave-number $r(K)$ for several values of d (w is still $0.25\lambda_R$). Note that the wave-number of surface wave is $r - K \sim -k_R$; thus the presented r describes the surface wave propagating and decaying in $-x$ direction. The decaying coefficient ($\text{Im}\{r\}$) grows with K but is quite small for small d . Although any extra damping of surface wave is unacceptable for applications in surface wave resonators, small damping at certain values of d is a promising feature for applications in comb transducers of surface waves.

Comb transducer is the system of vibrating teeth excited by the incident bulk waves (VIKTOROV, 1967). Typically, elevated teeth are applied (QUARRY, ROSE, 2002). When a comb is applied to the substrate, the vibrating teeth contribute to the transducer output by excitation of interface waves which propagate toward the transducer edges, where they are converted into surface waves (DANICKI, 2000a). It is essential for the transducer efficiency that the interface wave can collect ultrasonic energy on its propagation path under the transducer from all, even distant, teeth. This requires small interface wave damping caused by its

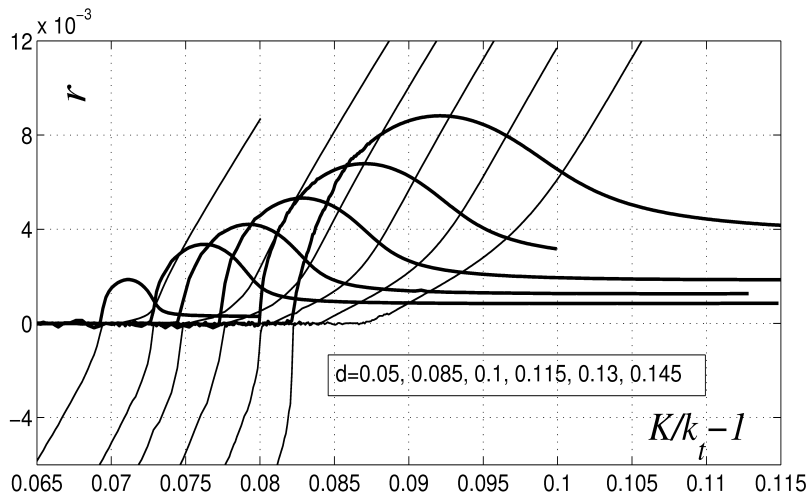


Fig. 4. Spatial frequency for $K \sim k_t$ and relatively small teeth height $d < w$; thin and thick lines present correspondingly $\text{Re}\{r\}$ and $\text{Im}\{r\}$. Small irregularities are caused by numerical inaccuracy.

leakage into bulk waves, in both the comb and the substrate. High damping would prevent the distant teeth contribution to the transducer output (DANICKI, 2002). In this paper, weak coupling of the comb to the substrate is assumed (QUARRY, ROSE, 2002) applying the idle comb approximation, hence considering the surface, instead of the interface waves. The results presented in Fig. 3 show that, contrary to common wisdom, small teeth height $d \sim \lambda_R/10$ may be advantageous for the transducer efficiency.

6. Conclusions

The analysis brings the following conclusions: 1) the application of elevated teeth for construction of Rayleigh wave Bragg reflectors is possible if the system is carefully designed for both the teeth height and period, one should be aware however that choosing large d does not automatically mean wider stopband and larger Bragg reflection, as they depend strongly on both d and the chosen teeth period $1/K$. 2) Applying teeth height above its width may not increase the reflection coefficient at all, 3) and even the Bragg reflection may vanish for very high teeth. 4) The applicable ‘proper Bragg reflection’ takes place within stopbands spanned between curves K_s of different slopes, governed by propagating plate modes of different polarization. 5) The analysis has shown that small teeth height may be advantageous for efficiency of comb transducers, where the teeth period approximately equals the Rayleigh wave-length, $K \sim k_R$. Moreover, in this case the perturbed surface wave spatial frequency $r \approx k_R$. This makes the wave-fields of both similarly decaying in the substrate, and this would reduce

their transformation loss at the transducer edges due to the mode mismatch (DANICKI, 2002).

Acknowledgment

The author acknowledges partial support by the State Committee for Scientific Research under Grant No. N-N 501-0072-33.

References

1. BESSERER H., MALISHEVSKY P.G. (2004), *Mode Series Expansion at Vertical Boundaries in Elastic Waveguides*, *Wave Motion*, **39**, 41–59.
2. BIRIUKOV S.V., GULYAEV YU.V., KRYLOV V.V., PLESSKY V.V. (1995), *Surface Acoustic Waves in Inhomogeneous Media* (Springer Series on Wave Phenomena), Springer, Berlin.
3. BREHOVSKICH L.N. (1957), *Waves in Layered Media* [in Russian], IAN, Moscow.
4. DANICKI E. (1984), *Perturbation theory of surface acoustic wave reflection from a periodic structure with arbitrary angle of incidence*, *Arch. Mech.*, **36**, 623–638.
5. DANICKI E. (2000a), *Periodic Crack-Model of Comb Transducers: Excitation of Interface Waves*, *Arch. Acoust.*, **25**, 213–227.
6. DANICKI E. (2000b), *Periodic Crack-Model of Comb Transducers: Efficiency and Optimization*, *Arch. Acoust.*, **25**, 487–507.
7. DANICKI E.J. (2002), *Scattering by periodic cracks and the theory of comb transducers*, *Wave Motion*, **35**, 355–370.
8. DANICKI E.J. (2008), *Evaluation of Planar Harmonic Impedance for Periodic Elastic Strips of Rectangular Cross Section by Plate Mode Expansion*, *ASME J. Appl. Mech.*, 041011-1–6.
9. GLASS N.E., MARADUDIN A.A. (1983), *Leaky surface-elastic waves on both flat and strongly corrugated surfaces for isotropic, nondissipative media*, *J. Appl. Phys.*, **54**, 796–805.
10. PAGNEUX V. (2006), *Revisiting the edge resonance for Lamb waves in a semi-infinite plate*, *J. Acoust. Soc. Am.*, **120**, 649–656.
11. QUARRY M.J., ROSE J.L. (2002), *Phase Velocity Spectrum Analysis for a Time Delay Comb Transducer for Guided Wave Mode Excitation*, Lawrence Livermore Nat. Lab. Preprint UCRL-JC-138500.
12. VIKTOROV I.A. (1967), *Rayleigh and Lamb Waves: Physical Theory and Applications*, Plenum Press, New York.